Supporting Information

Eco-foaming Lignin for Innovative Rigid Foams

Qiangu Yan [a], Timothy Ketelboeter [a], Wenjun Fan [b], Caixia Wan [b,*], and Zhiyong Cai [a,*]

[a] Forest Products Laboratory, USDA Forest Service, One Gifford Pinchot Drive, Madison, WI 53726-2398

[b] Department of Chemical and Biomedical Engineering, University of Missouri, 1406 East Rollins Street, Columbia, MO 65211

[*]Corresponding authors. Tel: +1 573 884 7882, Email: wanca@missouri.edu (Caixia Wan); Tel: +1 608-231-9446, Email: zhiyong.cai@usda.gov (Zhiyong Cai).

Numbers of Page: 12

Number of Table: 4

Number of Figure: 4

Supplementary Results

Assignment of bands in FTIR spectra of kraft lignin

Lignin contains various types of functional groups depending on lignocellulosic biomass species and isolation methods. Figure S1 shows a representative FTIR spectrum of raw kraft lignin used in the current work, and the assignments of common absorption bands are summarized in Table S1. A broad absorption peak in the range of 3700-3000 cm^{-1} is attributed to the –OH stretching of adsorbed moisture and hydroxyl groups (both phenolic and aliphatic).[1] The bands centered at 2934.8 cm^{-1} are associated with C–H stretching in methyl ($-CH_3$) and methylene ($=CH_2$) groups of the side chains.[2] The bands at 2842.7 cm^{-1} correspond to the C–H stretching of aromatic methoxy ($-OCH_3$) group.[1] The sample also shows the characteristic aromatic skeleton (phenylpropane unit) stretching vibrations at 1594.5, 1511.5, 1462.3 and 1426.9 cm^{-1},[3-6] and C–H bending vibration in the side chains of the phenylpropane unit at 1451.2 and 1366.4 cm^{-1}.[3] Other strong bands include those at 1699.1 cm^{-1} (C=O stretch, unconjugated ketone, carboxyl, and ester groups), 1265.1 cm^{-1} (asymmetric aryl ring stretching), 1207.7 cm^{-1} (asymmetric C–H deformation), 1266 cm^{-1} (aryl ring breathing), 1142.7 cm^{-1} (aromatic C-H in-plane deformations in guaiacyl units, secondary alcohols and C-O stretching), 1124.3 cm^{-1} (aromatic C-H in-plane deformations in guaiacyl units, secondary alcohols and C-O stretching), 1078.1 cm^{-1} (C-O deformation in secondary alcohols and aliphatic ethers), 1028.9 cm^{-1} (aromatic C–H in plane deformation), 853.4 cm^{-1} (C–H deformation of out of plane, aromatic ring), and 814.8 cm^{-1} (C–H deformation of out of plane, aromatic ring).[3]

Table S1. Moisture content of kraft lignin dried at different temperatures.

Drying Temperature (°C)	**Moisture Content (wt%)**
25	7.4±0.21
50	4.5±0.15
75	2.2±0.16
100	1.4±0.11
125	0.5±0.08
150	0

Table S2. Assignment of bands in FTIR spectra of kraft lignin

Bands (cm^{-1})	**Assignment**	**Ref.**
3345.9	O–H stretch, H-bonded	[1]
2934.8	C–H stretch on methyl and methylene groups	[2]
2842.7	C-H Stretch in methyl and methylene groups	[1]
1699.1	C=O stretch, unconjugated ketone, carboxyl, and ester groups	[7]
1652.3	Bending of H-O-H groups, absorbed water	[8]
1594.5	Aromatic skeletal vibrations plus C = O stretch	[3, 6]
1511.5	Aromatic skeletal vibrations of lignin and C=O stretching	[3, 6]
1462.3	C-H deformations; asymmetric $-CH_3$ and $-CH_2-$ aromatic skeletal vibrations combined	[5]
1451.2	C-H deformations; asymmetric $-CH_3$ and $-CH_2-$	[3, 9]
1426.9	Aromatic skeletal vibration combined with C–H in plane deformation	[3, 5]
1366.4	Aliphatic C-H Stretch in CH_3, not in OMe; phenolic OH	[3]
1265.1	Guaiacyl ring vibrations and C-O stretching	[3]
1207.7	C–C, C–O stretching	[3]
1142.7	Aromatic C-H in-plane deformations in guaiacyl units and secondary alcohols, and C-O stretching	[3]
1124.3	Aromatic C-H in-plane deformations in guaiacyl units and secondary alcohols and C-O stretching	[3]
1078.1	C-O deformation in secondary alcohols and aliphatic ethers	[3]
1028.9	aromatic C-H in-plane deformation	[3, 8]
853.4	C–H deformation of out of plane, aromatic ring	[3]
814.8	C–H deformation of out of plane, aromatic ring	[3]

Table S3. Assignment of the FTIR (ν_{OH}) bands of kraft lignin

Wavenumber of bands (cm^{-1})	**Band assignment**	**Ref.**
3602.5	Weakly hydrogen-bonded water	[6, 9]
3555	Weakly adsorbed water or intramolecular hydrogen bond in a phenolic group	[4, 10, 11]
3496	Valence vibration of H-bonded OH groups or moderately H-bonded water	[12]
3372	Intramolecular H-bonded -OH stretching	[13]
3280	-OH intramolecular and intermolecular stretching modes	[14]
3149	Strongly H-bonded water	[3, 6]
1636	-OH bending in adsorbed water –OH bending affected by water absorption	[4, 8, 15]

Table S4. Comparison of rigid foams and lignin-based foams*

Substrates	Foams	Density (g/cm^3)	Compressive Strength (MPa)	Thermal conductivity ($W\ m^{-1}\ K^{-1}$)	Ref.
Lignin-based foam PU foam	Rigid foam	0.519	12.87		16
Fly ash, polyurea	Core material modified by surface coating of 10-40% polyurea	0.544-0.604	16.83-19.15		16
Fly ash, PU	Core material impregnated by PU	0.932	31.44		16
Expanded polystyrene foam (EPS)		0.562	2.99	0.33	17
Polystyrene	Rigid cellular polystyrene thermal insulation	0.012-0.048	0.035-0.414	0.55-0.76	18
PU	Rigid cellular PU thermal insulation	0.019-0.048	0.104-0.690	0.81-0.88	19
PU, polyisocyanurate	PU modified polyisocyanurate cellular plastic		6-15		20
Low density PU	PU foam		0.117		21
Lignin, PU	5-30% lignin incorporated PU foam	0.0314-0.0365	0.16-0.18	0.024 - 0.025	22
Lignin	100% lignin	0.18-0.7	7.3-30.16		23
Lignin	Flexible PU foam	0.058-0.095	0.018-0.055 (Modulus)		24
Lignin, PU	PU foam	0.042-0.044	0.19-0.30	0.0226-0.0345	25
Lignin	PU foam	0.0339-0.0422	0.102-0.202	0.0233-0.025	26
Lignin	Rigid PU foam	0.024-0.030	>0.12	0.017-0.030	27
Lignin, bio-polyol,		0.041-0.044		0.023	28
Lignin, polyether polyol		0.036-0.120	0.09-0.47	0.025-0.027	29
Lignin, bio-phenol formaldehyde		0.037-0.038	0.06-1.12		30

*PU: polyurethane

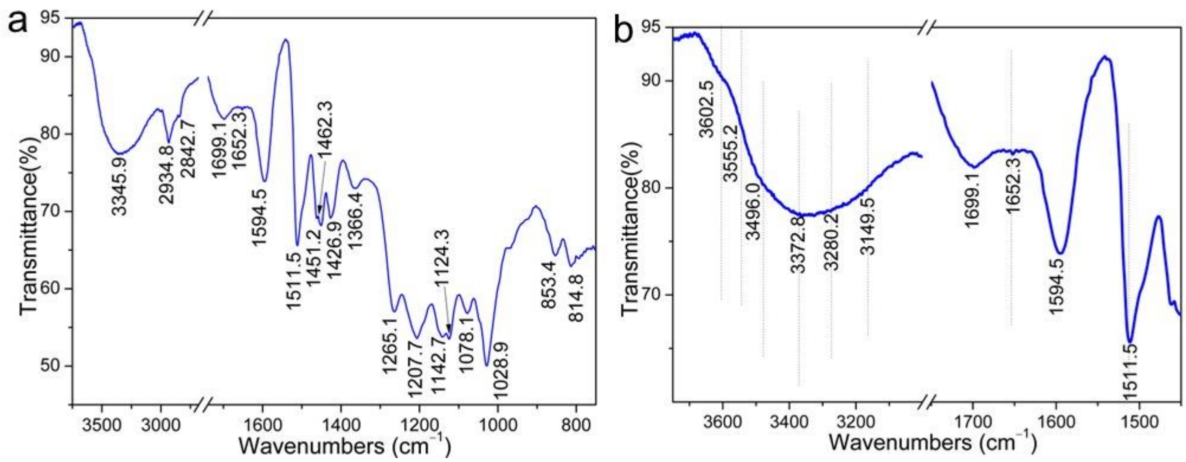

Figure S1. Typical Fourier-transform infrared (FTIR) spectra of raw kraft lignin.

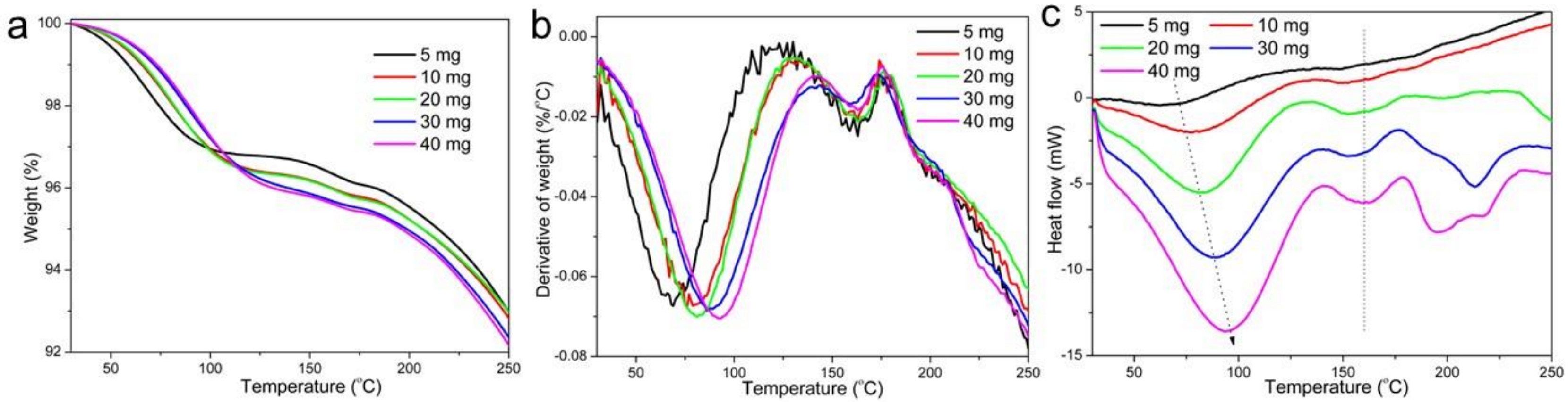

Figure 2. Effect of sample size on the thermal properties of kraft lignin sample (KL25) cold-pressed at 300 psi: (a) TG, (b) DTG, and (c) DSC.

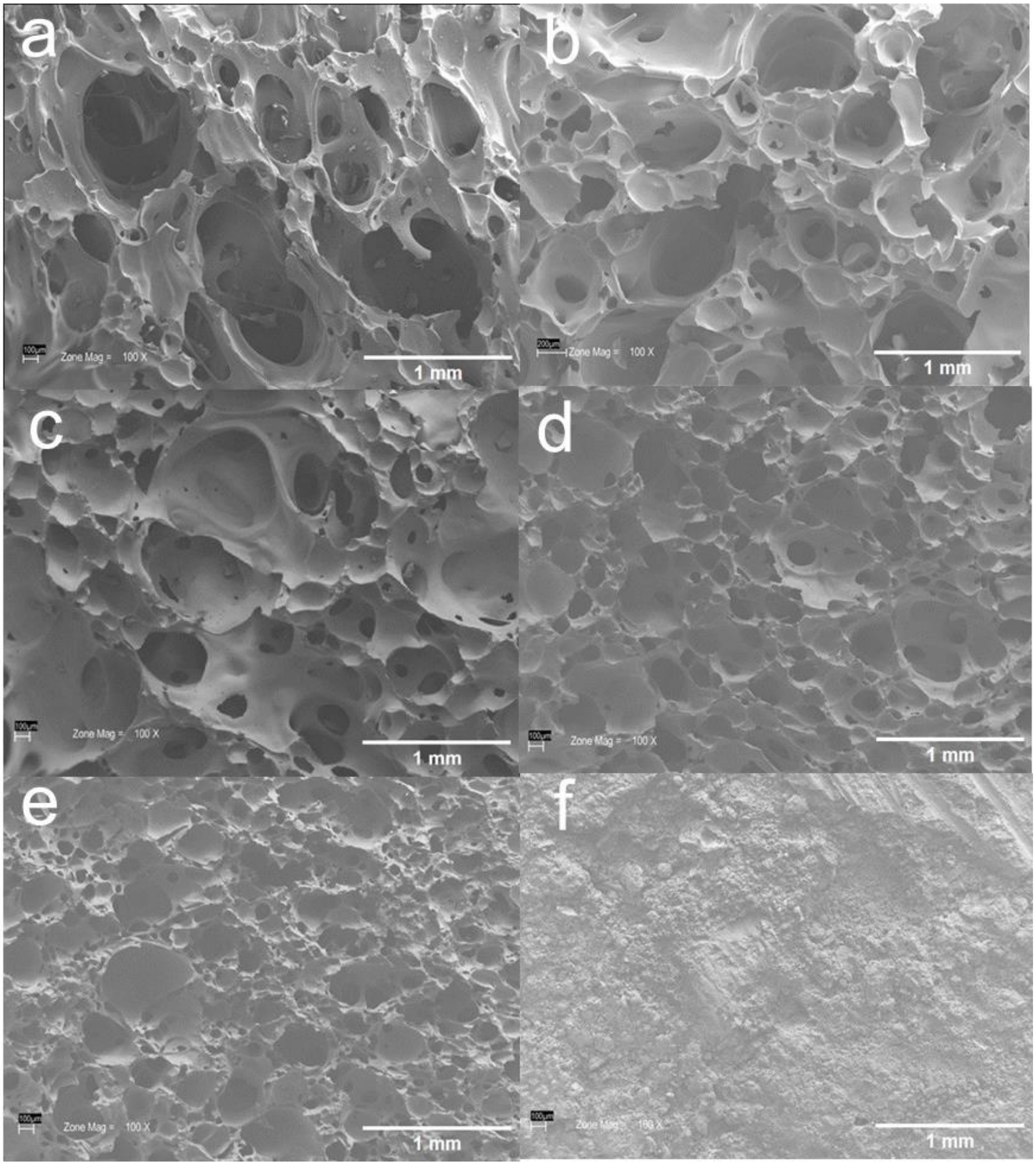

Figure S3. SEM images of foam under 100× magnification; (a) LF25, (b) LF50, (c) LF75, (d) LF100, (e) LF125, and (f) LF150.

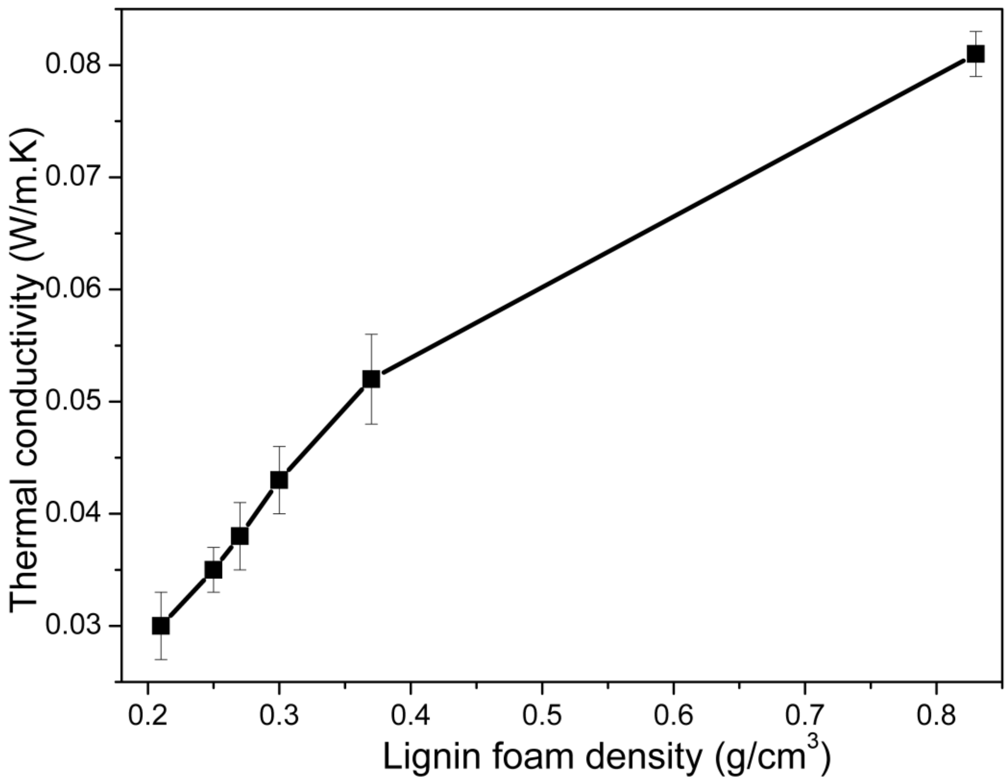

Figure S4. Correlation of lignin foam density and thermal conductivity.

References

1. M. Báder, R. Németh, J. Sandak and A. Sandak, *Cellulose*, 2020, **27**, 6811-6829.
2. S. M. Moosavinejad, M. Madhoushi, M. Vakili and D. J. M. C. y. t. Rasouli, 2019, **21**, 381-392.
3. O. Faix, *Holzforschung*, 1991, **45**, 21-28.
4. X. Guo, Y. Wu and N. Yan, *Wood Sci.*, 2018, **52**, 971-985.
5. N. Gierlinger, L. Goswami, M. Schmidt, I. Burgert, C. Coutand, T. Rogge and M. Schwanninger, *Biomacromolecules*, 2008, **9**, 2194-2201.
6. X. Guo, Y. Wu and N. Yan, *%J Wood Science*, 2018, **52**, 971-985.
7. M. Fodil Cherif, D. Trache, N. Brosse, F. Benaliouche and A. F. Tarchoun, *Waste Biomass Valorization*, 2020, **11**, 6541-6553.
8. M. Kačuráková, P. S. Belton, R. H. Wilson, J. Hirsch and A. Ebringerová, *J. Sci. Food Agric.*, 1998, **77**, 38-44.
9. J. R. Scherer, M. K. Go and S. Kint, *J. Phys. Chem.*, 1974, **78**, 1304-1313.
10. A. D. Pouwels, A. Tom, G. B. Eijkel and J. J. Boon, *J. Anal. Appl. Pyrolysis*, 1987, **11**, 417-436.
11. S. Kubo and J. F. Kadla, *Biomacromolecules*, 2005, **6**, 2815-2821.
12. M. Schwanninger, J. Rodrigues, H. Pereira and B. Hinterstoisser, *Vib. Spectrosc.*, 2004, **36**, 23-40.
13. O. Gordobil, R. Herrera, F. Poohphajai, J. Sandak and A. Sandak, *J. Mater. Res. Technol.*, 2021, **12**, 159-169.
14. C.-M. Popescu, G. Singurel, M.-C. Popescu, C. Vasile, D. S. Argyropoulos and S. Willför, *Carbohydr. Polym.*, 2009, **77**, 851-857.
15. J. P. McLean, G. Jin, M. Brennan, M. K. Nieuwoudt and P. J. Harris, *Can. J. For. Res.*, 2014, **44**, 820-830.
16. R. Panduranga, K. Shivakumar and L. Russell, presented in part at the 48th AIAA/ASME/ASCE/AHS/ASC Structures, Structural Dynamics, and Materials Conference, 2007.
17. A. Sariisik and G. Sariisik, *Materials and Structures*, 2012, **45**, 1345-1357.
18. ASTM-C578-23, 2023. Standard specification for rigid, cellular polystyrene thermal insulation.
19. ASTM-C1029-15, 2015. Standard specification forspray-applied rigid cellular polyurethane thermal insulation.
20. A. R. Kakroodi, M. Khazabi, K. Maynard, M. Sain and O.-S. Kwon, *Ind. Crops Prod.*, 2015, **74**, 1-8.
21. M. Mohamed, R. Hussein, A. Abutunis, Z. Huo, K. Chandrashekhara, L. Sneed and Materials, *J. Sandwich Struct. Mater.*, 2016, **18**, 769-789.
22. X. Zhang, Y. Kim, T. L. Eberhardt and R. Shmulsky, *Ind. Crops Prod.*, 2019, **132**, 292-300.
23. Q. Yan, R. Arango, J. Li and Z. Cai, *Mater. Des.*, 2021, **201**, 109460.
24. A. Gondaliya and M. Nejad, *Molecules*, 2021, **26**, 2302.
25. H. Haridevan, M. S. McLaggan, D. A. Evans, D. J. Martin, T. Seaby, Z. Zhang and P. K. Annamalai, *ACS Appl. Polym. Mater.*, 2021, **3**, 3528-3537.
26. X. Zhang, D. Jeremic, Y. Kim, J. Street and R. Shmulsky, *Polymers*, 2018, **10**, 706.

27. H. Haridevan, D. A. Evans, A. J. Ragauskas, D. J. Martin and P. K. Annamalai, *Green Chem.*, 2021, **23**, 8725-8753.
28. M. Kurańska, J. Pinto, K. Salach, M. Barreiro and A. Prociak, *Ind. Crops Prod.*, 2020, **143**, 111882.
29. A. N. Hayati, D. A. C. Evans, B. Laycock, D. J. Martin and P. K. Annamalai, *Ind. Crops Prod.*, 2018, **117**, 149-158.
30. B. Li, Z. Yuan, J. Schmidt and C. C. Xu, *Eur. Polym. J.*, 2019, **111**, 1-10.